Laser Physics, Vol. 15, No. 1, 2005, pp. 135–145.

Quantum Electrodynamics in Media with Negative Refraction[1]

J. Kästel and M. Fleischhauer*
Fachbereich Physik, Technische Universität Kaiserslautern, D-67663 Kaiserslautern, Germany
*e-mail: mfleisch@physik.uni-kl.de
Received September 17, 2004

Abstract—We consider the interaction of atoms with the quantized electromagnetic field in the presence of materials with negative indices of refraction. Spontaneous emission of an atom embedded in a negative-index material is discussed. It is shown, furthermore, that the possibility of a vanishing optical path length between two spatially separated points provided by these materials can lead to complete suppression of spontaneous emission of an atom in front of a perfect mirror even if the distance between the atom and the mirror is large compared to the transition wavelength. Two atoms put in the focal points of a lens formed by a parallel slab of an ideal negative-index material are shown to exhibit perfect sub- and superradiance. The maximum length scale in both cases is limited only by the propagation distance within the free-space radiative decay time. Limitations of the predicted effects that arise from absorption and the finite transversal extension and dispersion of the material are analyzed.

1. INTRODUCTION

Since the early days of quantum electrodynamics, it has been well known and appreciated that the radiative decay of an isolated atom, as well as the radiative interaction between different atoms, can be strongly affected by the environment. As was first noted by E.M. Purcell [1, 2], the presence of conducting walls can strongly accelerate or suppress spontaneous emission. Inhibited emission [3], enhanced decay [4], and the suppression of blackbody absorption [5, 6] have been observed with Rydberg atoms in cavity systems. Alterations of the spontaneous emission rate have also been observed near dielectric interfaces [7] and in quantum-well structures [8]. Furthermore, photonic bandgap materials with an engineered density of states of the radiation field can lead to suppression or acceleration of spontaneous decay [9, 10].

In this paper we discuss QED effects of single atoms and pairs of atoms in the presence of artificial materials showing negative refraction. Negative-index materials were first predicted by V. Veselago [11], who showed that simultaneous negative values of the dielectric permittivity ε and the magnetic permeability μ imply a negative index of refraction. These so-called left-handed materials attracted much attention when J. Pendry noticed that the possibility of a vanishing optical path length between two separated points using media with a negative index of refraction allows for a perfect lens with a resolution not limited by diffraction [12]. Such a lens, formed by an infinite parallel slab of lossless left-handed material of thickness d, collects all plane waves from a point source on one side of the slab in a focal point on the other side. If the refractive index of the material is $n = -1$, the distance between the two focal points is $2d$, while the optical path between them vanishes. We will show here that the same effect can lead to a drastic modification of the radiative decay of a two-level atom placed in front of a conducting surface (the Purcell effect) and to the radiative interaction between two atoms even if the involved distances are large compared to the resonance wavelength. We show that spontaneous emission from an atom at a distance $2d$ from the surface of a perfect mirror can be completely suppressed for dipole orientations in the plane of the mirror, if the space between the atom and the mirror contains a slab of $n = -1$ material with thickness d. Thanks to this, an effect otherwise occurring only within a distance that is small compared to the transition wavelength would become observable for macroscopic distances. We will show furthermore that two atoms put into the focal points of an ideal Veselago–Pendry lens behave as if both were at the same position; i.e., they show perfect Dicke sub- and superradiance [13].

After summarizing the basic properties of left-handed materials and analyzing the conditions for their existence for the case of realistic, i.e., causal and in general lossy magnetodielectrics in Section 2, we will discuss the alteration of the spontaneous emission rate of an atom embedded in a left-handed material in Section 3. It will be shown that the modification of the spontaneous emission rate due to the changed density of states is no longer given by the index of refraction n as in dielectric materials [14], but by the product μn, which remains positive also for lossless negative-index materials [15]. In Section 4, we will then analyze the radiative decay of a single two-level atom in front of a perfect mirror with a layer of negative-index material, as well as the radiative coupling of two atoms in the focal points of a Veselago–Pendry lens in Section 5. Finally, in Section 6 we will discuss limitations due to finite

[1] This paper is dedicated to the 70th birthday of Herbert Walther, whose pioneering experimental work on cavity quantum electrodynamics with Rydberg atoms has sharpened our understanding of the fundamentals of light–matter interaction.

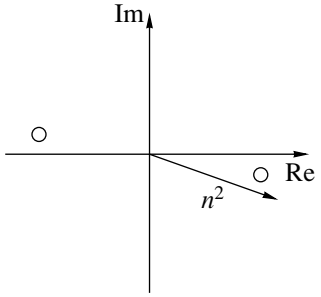

Fig. 1. n^2 for Re[ε], Re[μ] both being negative. The two possible complex square roots are indicated by circles.

absorption, to a finite transversal extension of the lens, and to dispersion, which necessarily accompanies negative refraction.

2. ELECTRODYNAMICS OF MEDIA WITH NEGATIVE REFRACTIVE INDICES

Macroscopic electrodynamics in linear isotropic media is completely characterized by two material functions, namely, dielectric permittivity ε and magnetic permeability μ. ε and μ relate the vector of the polarization **P** to that of the electric field **E** and, correspondingly, the vector of magnetization **M** to that of the magnetic field **B**. The most general expressions for **P** and **M** in linear isotropic magnetodielectrics read as follows:

$$\mathbf{P}(\mathbf{r}, t) = \varepsilon_0 \int_{-\infty}^{\infty} d\tau \chi_D(\mathbf{r}, \tau)\mathbf{E}(\mathbf{r}, t-\tau) \quad (1)$$

and

$$\mathbf{M}(\mathbf{r}, t) = \kappa_0 \int_{-\infty}^{\infty} d\tau \chi_M(\mathbf{r}, \tau)\mathbf{B}(\mathbf{r}, t-\tau), \quad (2)$$

where $\kappa_0 = 1/\mu_0$. χ_D and χ_M are the electric and magnetic susceptibilities, respectively. For causality, the susceptibilities have to be zero for $\tau < 0$. The dielectric permittivity $\varepsilon(\omega)$ then reads

$$\varepsilon(\mathbf{r}, \omega) = 1 + \int_0^{\infty} d\tau \chi_D(\mathbf{r}, \tau) e^{i\omega\tau}. \quad (3)$$

Correspondingly, the magnetic permeability $\mu = 1/\kappa$ is given by

$$\kappa(\mathbf{r}, \omega) = 1 - \int_0^{\infty} d\tau \chi_M(\mathbf{r}, \tau) e^{i\omega\tau}. \quad (4)$$

Causality requires that the poles of $\varepsilon(\omega)$ and $\mu(\omega)$ are in the lower half of the complex plane. $\varepsilon(\omega)$ and $\mu(\omega)$ usually have a resonance structure in ω-space, e.g.,

$$\varepsilon(\omega) = 1 + \frac{\omega_{Pe}^2}{\omega_{Te}^2 - \omega^2 - i\omega\gamma_e} \quad (5)$$

and

$$\mu(\omega) = 1 + \frac{\omega_{Pm}^2}{\omega_{Tm}^2 - \omega^2 - i\omega\gamma_m}. \quad (6)$$

For a sufficient strength of the resonance, i.e., for ω_{Pe}, ω_{Pm} being large, both Re[ε] and Re[μ] may become negative for certain frequencies.

Suppose that, at a particular frequency, $\varepsilon = \mu = -1$ holds. Then, the question arises: what are the implications for the refractive index $n(\mathbf{r}, \omega)$? From the definition of $n(\mathbf{r}, \omega)$

$$n(\mathbf{r}, \omega)^2 = \varepsilon(\mathbf{r}, \omega) \cdot \mu(\mathbf{r}, \omega), \quad (7)$$

one might conclude

$$n = \sqrt{\varepsilon \cdot \mu} = \sqrt{(-1)\cdot(-1)} = \sqrt{1} = 1. \quad (8)$$

However, as pointed out by Veselago [11], since ε and μ are complex functions, one has to decide which complex root to take. Noting that the imaginary part of $n(\mathbf{r}, \omega)$ characterizes the absorption of the medium, for a passive medium $\mathrm{Im}[n(\mathbf{r}, \omega)] \geq 0$ should hold, which fixes the root. As can be seen from Fig. 1, the correct choice is

$$n(\mathbf{r}, \omega) = \sqrt{|\varepsilon(\mathbf{r}, \omega)| \cdot |\mu(\mathbf{r}, \omega)|} \times \exp\left[+\frac{i}{2}\left(\operatorname{arccot}\frac{\varepsilon_R(\mathbf{r}, \omega)}{\varepsilon_I(\mathbf{r}, \omega)} + \operatorname{arccot}\frac{\mu_R(\mathbf{r}, \omega)}{\mu_I(\mathbf{r}, \omega)}\right)\right]. \quad (9)$$

Here, ε_R, μ_R and ε_I, μ_I denote the real and imaginary parts of ε and μ, respectively. With this one finds the following for the case of $\varepsilon = \mu = -1$:

$$n = \lim_{\varepsilon_I, \mu_I \to 0} \exp\left[\frac{i}{2}\left(\operatorname{arccot}\frac{-1}{\varepsilon_I} + \operatorname{arccot}\frac{-1}{\mu_I}\right)\right] = -1. \quad (10)$$

It is easy to see from Eq. (9) that a negative real part of the refractive index occurs if and only if [16]

$$\pi \geq \operatorname{arccot}\left(\frac{\varepsilon_R}{\varepsilon_I}\right) + \operatorname{arccot}\left(\frac{\mu_R}{\mu_I}\right) > \pi/2. \quad (11)$$

In Fig. 2, we have illustrated the frequency dependence of the index of refraction for the single-resonance model given in Eqs. (5) and (6). For frequencies around $\omega = 1.05\omega_{Te}$, the negativity of Re[n] is clearly recognizable.

The example in Fig. 2 shows a strong dispersion of the material functions $\varepsilon(\omega)$ and $\mu(\omega)$. In fact, as was pointed out already by Veselago, this is a general property of negative-index materials. Considering the

energy of the electromagnetic field in a nondispersive medium,

$$w = \varepsilon \mathbf{E}^2 + \mu \mathbf{H}^2, \tag{12}$$

one recognizes that negative values of ε and μ would lead to a negative energy. Therefore, a negative index of refraction is necessarily associated with dispersion, in which case the energy of the electromagnetic field reads

$$w = \mathrm{Re}\left[\frac{d(\omega\varepsilon)}{d\omega}\right]\mathbf{E}^2 + \mathrm{Re}\left[\frac{d(\omega\mu)}{d\omega}\right]\mathbf{H}^2, \tag{13}$$

which is positive even for negative ε and μ if the dispersion is normal and sufficiently large, such that

$$\mathrm{Re}\left[\frac{d(\omega\varepsilon)}{d\omega}\right] \geq 0, \quad \text{and} \quad \mathrm{Re}\left[\frac{d(\omega\mu)}{d\omega}\right] \geq 0. \tag{14}$$

In the following, we want to discuss some of the peculiar aspects of light propagation in negative-index materials. Making use of the boundary conditions between media with positive and negative refractive indices, namely, $\mathbf{E}^{\perp}$ and $\mathbf{H}^{\perp}$ being continuous, as are $\mathbf{D}^{\parallel}$ and $\mathbf{B}^{\parallel}$, one finds that an incident plane wave is refracted to the same side of the normal, as shown in Fig. 3. This behavior is fully consistent with Snell's law:

$$\frac{n_2}{n_1} = \frac{\sin(\alpha)}{\sin(\beta)}. \tag{15}$$

One striking feature of negative refraction is that the wave vector of the refracted wave $\mathbf{k}^r$ points backward, which is due to conservation of momentum parallel to the surface. As a result, the vectors **k**, **E**, **H** form a left-handed tripod instead of the usual right-handed one. Materials with a negative index of refraction are, therefore, also called left-handed media (LHM).

On the other hand, the Poynting vector $\mathbf{S} = \mathbf{E} \times \mathbf{H}$ clearly forms a right-handed tripod with **E** and **H** and, therefore, points in the correct direction, namely, away from the surface, as it should be due to conservation of energy (dashed arrows in Fig. 3).

Besides strong influences on the Doppler and Cherenkov effects [11], the most prominent effect of the negative refraction is probably the so-called perfect lens formed by a slab of a LHM. It was Veselago [11] who, when first studying the properties of lenses formed by a left-handed material, found that an infinitely extended slab of a LHM collects, in a focal point on the other side of the slab, all plane waves coming from a point source not too far away from the surface (Fig. 4). For a slab of thickness d, the distance between the two focal points is $d(1-n)$, where n is the refractive index of the LHM. Noting that the optical path length between points P_1 and P_2 is

$$l^{\mathrm{opt}} = (d(1-n)-d) + nd = 0, \tag{16}$$

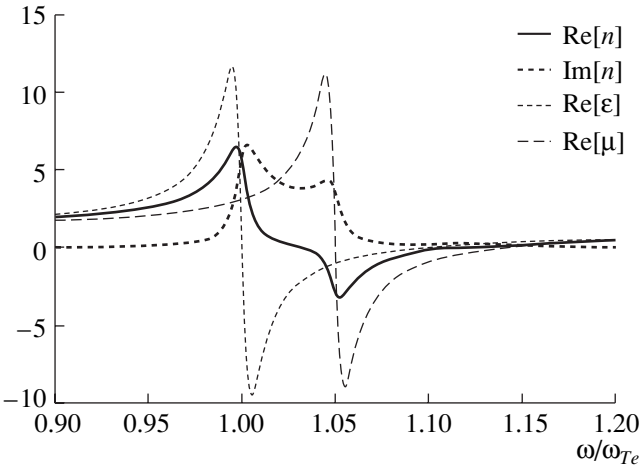

Fig. 2. Re[$n(\omega)$], Im[$n(\omega)$], Re[$\varepsilon(\omega)$] and Re[$\mu(\omega)$] using Eqs. (5) and (6). Parameters: $\omega_{Pe} = \omega_{Pm} = 0.46\omega_{Te}$; $\omega_{Tm} = 1.05\omega_{Te}$; $\gamma_e = \gamma_m = 0.01\omega_{Te}$.

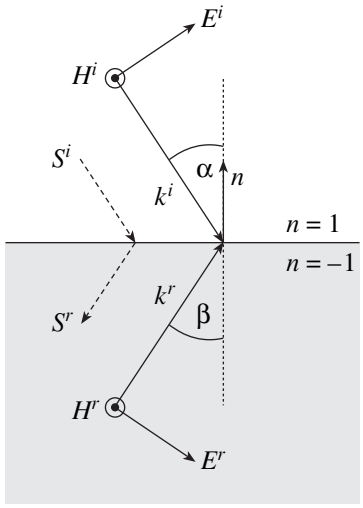

Fig. 3. Boundary between positive and negative refraction. In a material with a negative refractive index, the refracted wave goes to negative angles.

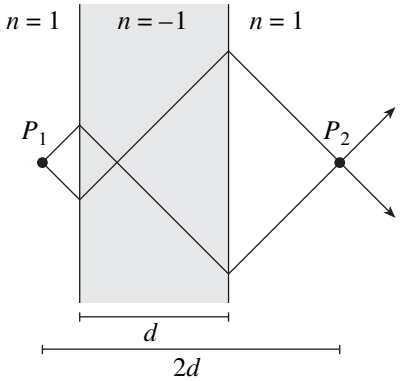

Fig. 4. Perfect lens formed by a infinitely extended slab of a LHM. The optical length between the foci P_1 and P_2 is zero.

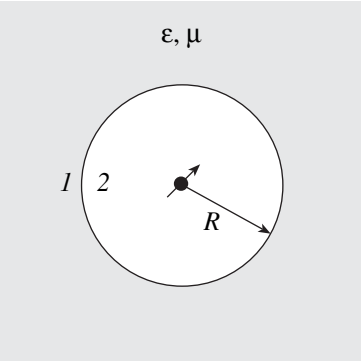

Fig. 5. Real-cavity model: the atom is located at the center of an empty cavity surrounded by the dielectric body.

the perfection of the lens becomes clear. The lens simulates a situation in which point P_2 is at the same spatial position as point P_1. When traveling a zero path, no information about the source can get lost, including that contained in the evanescent waves. Therefore, the perfect lens allows an unlimited resolution of the source [12].

3. SPONTANEOUS EMISSION OF AN ATOM EMBEDDED IN A MEDIUM WITH NEGATIVE REFRACTION

It is a well known fact that the natural linewidth Γ of a dipole allowed transition is not an intrinsic feature of an atom, but rather depends on the local environment. Based on an analysis of the density of states of the radiation field, Nienhuis and Alkemade predicted the following for an atom embedded in a homogeneous transparent dielectric with refractive index n [14]:

$$\Gamma = \Gamma_0 n, \tag{17}$$

where Γ_0 is the free-space decay rate:

$$\Gamma_0 = \frac{d^2\omega_A^3}{3\pi\hbar\varepsilon_0 c^3}, \tag{18}$$

where d is the dipole moment and ω_A is the atomic transition frequency. It was seen later that Eq. (17) does not give the correct behavior of Γ, since the macroscopic description of the surrounding medium fails in the immediate environment of the probe atom. To correct this in leading order of the medium density, local-field corrections need to be included. Several models have been established for this. The one that best describes a substitutive probe atom in a cubic-lattice host is the so-called real-cavity model [17], in which

$$\Gamma = n\Gamma_0 \mathcal{L}_{\text{real}}^2. \tag{19}$$

Here, $\mathcal{L}_{\text{real}} = 3\varepsilon/(2\varepsilon + 1)$ is the Glauber–Lewenstein factor, which accounts for near-field effects. This model assumes the atom to be located at the center of a small empty cavity surrounded by the dielectric body, which is treated macroscopically (see Fig. 5).

When considering atoms embedded in negative-index materials, Eqs. (17) and (19) are obviously not correct, since Γ would become negative in this case. This is because these expressions are derived only for dielectric surroundings [17, 18], where the contribution of the magnetic dipoles of the material was neglected.

Following Fermi's golden rule, the rate of spontaneous emission of an electric dipole transition is given by the imaginary part of the retarded Green function $\mathbf{G}$ of the electric field at the position $\mathbf{r}_A$ of the atom and at the transition frequency ω_A [15]:

$$\Gamma = \frac{2\omega_A^2 d_i d_j}{\hbar\varepsilon_0 c^2}\text{Im}[G_{ij}(\mathbf{r}_A, \mathbf{r}_A, \omega_A)]. \tag{20}$$

Here, d_i is the Cartesian ith component of the dipole moment. The influence of the surroundings on the mode structure is contained in the Green tensor $\mathbf{G}$. Thus, in order to include the effect of the magnetic dipoles of the left-handed medium, the Green tensor needs to be calculated for the case of a magnetodielectrics. Thus, the solution of the equation

$$\left(\nabla_{\mathbf{r}} \times [\kappa(\mathbf{r}, \omega)\nabla_{\mathbf{r}}\times] - \frac{\omega^2}{c^2}\varepsilon(\mathbf{r}, \omega)\right)\mathbf{G}(\mathbf{r}, \mathbf{r}', \omega) = \delta(\mathbf{r} - \mathbf{r}')\mathbf{1} \tag{21}$$

needs to be determined for given boundary conditions. Note the term $\kappa(\mathbf{r}, \omega) = 1/\mu(\mathbf{r}, \omega)$, which is absent in the pure dielectric case [18].

Since within the Glauber–Lewenstein model the atom is located in free space, the solution of Eq. (21) for the real cavity (Fig. 5) can be expressed as a sum of the free-space Green function and a scattering term that accounts for the boundary of the magnetodielectric:

$$\mathbf{G}(\mathbf{r}, \mathbf{r}') = \mathbf{G}^{\text{vac}}(\mathbf{r}, \mathbf{r}') + \mathbf{G}^{s}(\mathbf{r}, \mathbf{r}') \quad |\mathbf{r}|, |\mathbf{r}'| < R, \tag{22}$$

with

$$\text{Im}[\mathbf{G}_{ij}^{\text{vac}}(\mathbf{r}, \mathbf{r}, \omega)] = \frac{k}{6\pi}\delta_{ij}, \quad k = \omega/c \tag{23}$$

and

$$\mathbf{G}^{s}(\mathbf{r}, \mathbf{r}') = \frac{ik}{4\pi}\sum_{n=1}^{\infty}\sum_{m=0}^{n}\sum_{l=e,o}(2 - \delta_{0m}) \times \frac{2n+1}{n(n+1)}\frac{(n-m)!}{(n+m)!}[\mathcal{C}_M^n(k)\mathbf{M}_{lmn}(\mathbf{r}, k)\mathbf{M}_{lmn}(\mathbf{r}', k) + \mathcal{C}_N^n(k)\mathbf{N}_{lmn}(\mathbf{r}, k)\mathbf{N}_{lmn}(\mathbf{r}', k)]. \tag{24}$$

Due to the symmetry of the geometry, the scattering term can be expanded in a series of vector Bessel functions:

$$\mathbf{M}_{lmn}(\mathbf{r}, k) = \nabla \times [\psi_{lmn}(\mathbf{r}, k)\mathbf{r}], \quad (25)$$

$$\mathbf{N}_{lmn}(\mathbf{r}, k) = \frac{1}{k}\nabla \times \nabla \times [\psi_{lmn}(\mathbf{r}, k)\mathbf{r}], \quad (26)$$

$$\psi_{lmn}(\mathbf{r}, k) = j_n(kr)P_n^m(\cos\theta)f_l(m\phi), \quad (27)$$

where f_l has the meaning of a cosine function for even l and of a sine function for odd l. The j_n are spherical Bessel functions of the first kind, and the P_n^m are the associated Legendre polynomials. The rather lengthy expansion factors $\mathcal{C}_N^n(k)$ and $\mathcal{C}_M^n(k)$ are given in [19].

In the limit $\mathbf{r}, \mathbf{r}' \longrightarrow 0$, all terms except that with $\mathcal{C}_N^1$ become zero. The rate of spontaneous emission of a two-level atom embedded in a medium of arbitrary ε and μ then reads

$$\Gamma = \Gamma_0(1 + \mathrm{Re}[\mathcal{C}_N^1(\omega_A)]), \quad (28)$$

with

$$\mathcal{C}_N^1(\omega_A) = e^{i\varrho}\left[i + \varrho(n+1) - i\varrho^2 n(n+1)\frac{\mu - n}{\mu - n^2} - \varrho^3 n^2 \frac{\mu - n}{\mu - n^2}\right] \times \left[i\varrho^2 n\left(\cos\varrho + in\frac{\mu - 1}{\mu - n^2}\sin\varrho\right) - \varrho(\cos\varrho + in\sin\varrho) \times \sin\varrho + \varrho^3(\mu\cos\varrho - in\sin\varrho)\frac{n^2}{\mu - n^2}\right]^{-1}. \quad (29)$$

Here, $\varrho = \frac{R\omega_A}{c}$ is the normalized radius of the cavity. This function can be shown to be strictly positive, as it should be for the rate of spontaneous emission. In the limit of vanishing imaginary parts of μ, ε, and n, Eq. (28) reduces to

$$\Gamma = n\mu\Gamma_0\left(\frac{3\varepsilon}{2\varepsilon + 1}\right)^2, \quad (30)$$

which is the sought generalization of the formula of Glauber and Lewenstein (Eq. (19)) for pure dielectrics in the case of lossless but otherwise arbitrary magnetodielectric media. For $\mu = 1$, Eq. (30) reduces to the dielectric case.

The influence of the LHM on the rate of spontaneous emission for a resonance model using the example of Eqs. (5) and (6) is shown in Fig. 6. Because of the surrounding medium, the natural linewidth in the vicinity of the resonance can be either strongly enhanced or suppressed.

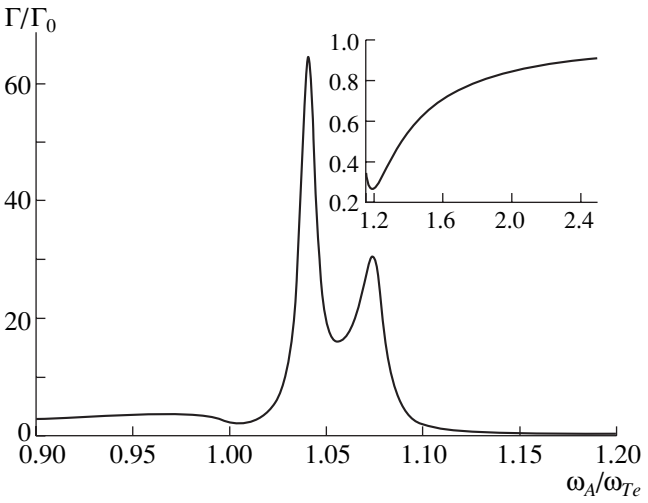

Fig. 6. Rate of spontaneous emission for the real-cavity model for resonant functions (5) and (6). $\omega_{Pe} = \omega_{Pm} = 0.46\omega_{Te}$; $\omega_{Tm} = 1.05\omega_{Te}$; $\gamma_e = \gamma_m = 0.01\omega_{Te}$.

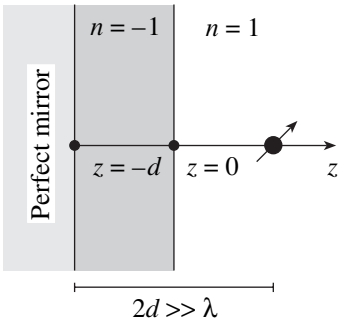

Fig. 7. Atom in front of a LHM attached to a mirror. The optical length between the atom and the mirror is zero. The spatial regions $z > 0$, $-d \le z \le 0$, and $z < -d$ are denoted by the numbers 0, 1, and 2, respectively.

4. SUPPRESSION OF SPONTANEOUS EMISSION OF AN ATOM IN FRONT OF A MIRROR: MODIFIED PURCELL EFFECT

In this section, the modification of the Purcell effect, i.e., the suppression of the spontaneous emission of an atom in front of a mirror by a medium with negative refraction, will be discussed. For this, we consider the setup shown in Fig. 7. The atom is placed at a distance $2d$ from the surface of the perfect mirror, and the space between the atom and the mirror is filled half by a vacuum and half by a medium with $n = -1$. In the absence of the medium, the emission rate of the atom is significantly affected only if the distance between the atom and the mirror is small compared to the transition wavelength [20]. In this case, the radiative decay for a transition with a dipole moment parallel to the plane of the mirror vanishes, while that for an orthogonal dipole moment is enhanced by a factor of two. Since, in the

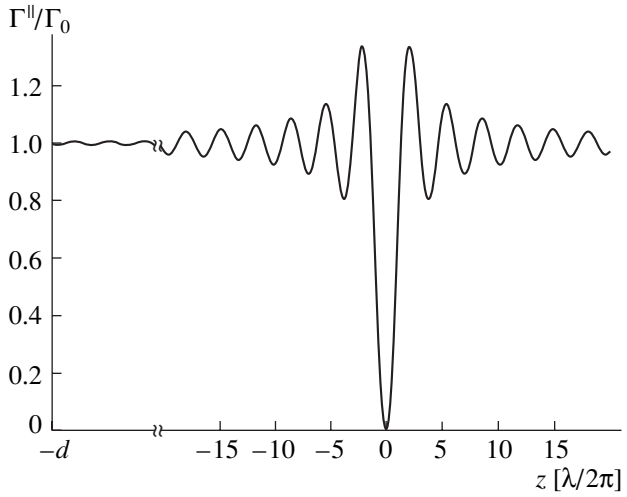

Fig. 8. Spatial dependence of the normalized rate of spontaneous emission $\Gamma^{\parallel}(z)/\Gamma_0$ for a dipole parallel to the mirror surface. z is the spatial shift in the z direction of the atom out of its focus; d is the distance from the focus to the surface of the LHM.

presence of the negative-index material, as in Fig. 7, the optical length of the path from the atom to the mirror equals zero, the question arises as to whether the LHM leads to properties comparable to the case of the atom sitting on the mirror surface. To obtain an answer to this, we note that the rate of spontaneous emission of an atom in a linear and isotropic, but otherwise arbitrary, environment is given by Eq. (20). Thus, we only need to calculate the Green function corresponding to the specific setup.

The retarded Green function corresponding to a slab with a homogeneous and linear magnetodielectric medium can be calculated by a plane-wave decomposition. Following [21], one finds, for the two positions $\mathbf{r}$ and $\mathbf{r}'$ in vacuum on the same side of the slab,

$$\begin{aligned}\mathbf{G}^{00}(\mathbf{r}, \mathbf{r}', \omega) &= \frac{i}{8\pi^2}\int d^2k_\perp \frac{1}{k_z}[(R^{\mathrm{TE}}\hat{\mathbf{e}}(k_z)e^{i\mathbf{k}\cdot\mathbf{r}} \\ &\quad + \hat{\mathbf{e}}(-k_z)e^{i\mathbf{K}\cdot\mathbf{r}}) \circ \hat{\mathbf{e}}(-k_z)e^{-i\mathbf{K}\cdot\mathbf{r}'} \\ &+ (R^{\mathrm{TM}}\hat{\mathbf{h}}(k_z)e^{i\mathbf{k}\cdot\mathbf{r}} + \hat{\mathbf{h}}(-k_z)e^{i\mathbf{K}\cdot\mathbf{r}}) \circ \hat{\mathbf{h}}(-k_z)e^{-i\mathbf{K}\mathbf{r}'}],\end{aligned} \tag{31}$$

where $z \le z'$ has been assumed. Since it is needed later, we also give the Green function for the case in which $\mathbf{r}$ and $\mathbf{r}'$ are in vacuum on different sides of the slab:

$$\begin{aligned}&\mathbf{G}^{20}(\mathbf{r}, \mathbf{r}', \omega) \\ &= \frac{i}{8\pi^2}\int d^2k_\perp \frac{1}{k_z}[T^{\mathrm{TE}}\hat{\mathbf{e}}(-k_z)e^{i\mathbf{K}\cdot\mathbf{r}} \circ \hat{\mathbf{e}}(-k_z)e^{-i\mathbf{K}\cdot\mathbf{r}'} \\ &\quad + T^{\mathrm{TM}}\hat{\mathbf{h}}(-k_z)e^{i\mathbf{K}\cdot\mathbf{r}} \circ \hat{\mathbf{h}}(-k_z)e^{-i\mathbf{K}\mathbf{r}'}].\end{aligned} \tag{32}$$

The superscripts 0, 1, 2 in the Green functions denote the position zones of $\mathbf{r}$ and $\mathbf{r}'$: $z > 0$, $-d \le z \le 0$, and $z < -d$, respectively. For later convenience, $\mathbf{G}^{20}$ is given under the assumption of medium 2 being a vacuum. We here have used the definitions $k^2 = \omega^2/c^2$, $k_z = \sqrt{k^2 - k_\perp^2}$, and $d^2k_\perp = dk_x dk_y$. Furthermore, $\mathbf{K} \equiv k_x\hat{\mathbf{x}} + k_y\hat{\mathbf{y}} - k_z\hat{\mathbf{z}}$, and we have introduced the orthogonal unit vectors $\hat{\mathbf{e}} = \mathbf{k}\times\hat{\mathbf{z}}/|\mathbf{k}\times\hat{\mathbf{z}}|$ and $\hat{\mathbf{h}} = p\hat{\mathbf{e}}\times\mathbf{k}/|k|$, where $p = 1$ for a normal medium and $p = -1$ for a LHM. R^{TE}, R^{TM} and T^{TE}, T^{TM} are the reflection and transmission functions of the three-layer medium for transverse-electric and transverse-magnetic modes. They read

$$R^{\mathrm{TE}} = \frac{R_{01} + R_{12}e^{i2k_{1z}d}}{1 + R_{01}R_{12}e^{i2k_{1z}d}}, \tag{33}$$

$$R^{\mathrm{TM}} = \frac{S_{01} + S_{12}e^{i2k_{1z}d}}{1 + S_{01}S_{12}e^{i2k_{1z}d}}, \tag{34}$$

and, correspondingly,

$$T^{\mathrm{TE}} = \frac{2\mu k_z}{\mu k_z + k_{1z}}\frac{1 + R_{12}}{1 + R_{01}R_{12}e^{i2k_{1z}d}}e^{i(k_{1z} - k_z)d}, \tag{35}$$

$$T^{\mathrm{TM}} = \frac{2\varepsilon k_z}{\varepsilon k_z + k_{1z}}\frac{1 + S_{12}}{1 + S_{01}S_{12}e^{i2k_{1z}d}}e^{i(k_{1z} - k_z)d}. \tag{36}$$

Here, $k_{1z} = \sqrt{k_1^2 - k_\perp^2}$ and $k_1^2 = \varepsilon(\omega)\mu(\omega)\omega^2/c^2$. R_{ij} and S_{ij} are the reflection coefficients at the boundaries between media i and j for the TE and TM modes, respectively:

$$R_{ij} = \frac{\mu_j k_{iz} - \mu_i k_{jz}}{\mu_j k_{iz} + \mu_i k_{jz}}, \quad S_{ij} = \frac{\varepsilon_j k_{iz} - \varepsilon_i k_{jz}}{\varepsilon_j k_{iz} + \varepsilon_i k_{jz}}. \tag{37}$$

Setting $R_{12} = -1$ and $S_{12} = 1$ to account for the perfect mirror, we obtain the natural linewidth by substituting the corresponding result for $\mathbf{G}^{00}$ into

$$\Gamma = \frac{2\omega_A^2 d_i d_j}{\hbar\varepsilon_0 c^2}\mathrm{Im}[\mathbf{G}_{ij}^{00}(\mathbf{r}_A, \mathbf{r}_A, \omega_A)]. \tag{38}$$

The result is shown in Fig. 8 for the case in which the atomic dipole moment is parallel to the surface of the mirror. The thickness of the LHM is set to $d = 100\dfrac{\lambda}{2\pi}$. When the atom is put at a distance d before the LHM, which we want to denote as the focal point, the rate of spontaneous emission is completely suppressed:

$$\Gamma^{\parallel}_{\mathrm{focus}} = 0. \tag{39}$$

The spatial dependence of the linewidth shown in Fig. 8 is the same as for an atom in front of a mirror located at $z = 0$ without a LHM [20]. For atomic dipoles with an orthogonal orientation to the mirror, the spatial dependence is also the same as in the case in which there is

no LHM, but where the mirror is at $z = 0$ (see [20]). In the focus, this leads to an enhancement of the decay rate by a factor of two:

$$\Gamma^{\perp}_{\text{focus}} = 2\Gamma_0. \tag{40}$$

The behavior shown in Fig. 8 can be understood in the following way: the combination of layers of vacuum ($n = +1$) and of negative-index material ($n = -1$) with equal thicknesses d makes the space between atom and mirror appear to be of zero (optical) length. Thus, the atom at the focal point is equivalent to the atom being on the mirror surface. This result suggests the possibility of experimentally studying spontaneous emission suppression of atoms near a mirror without the necessity of actually putting the atoms on the surface.

5. SUB- AND SUPERRADIANCE OVER MACROSCOPIC DISTANCES

The observation of the last section, namely, that a combination of a layer of positive and negative refraction can make a spatial volume appear to have a vanishing optical thickness, suggests a different interesting application. If two atoms are put at the focal points of a Veselago–Pendry lens, as indicated in Fig. 9, they should show a radiative coupling with a strength as if they were at the same position in space.

We now want to analyze this situation in detail. For this, we start with the interaction Hamiltonian of two atoms at positions $\mathbf{r}_1$ and $\mathbf{r}_2$ with the quantized electric field $\hat{\mathbf{E}}$ in the dipole and rotating-wave approximations:

$$H_{\text{WW}} = -\hat{\mathbf{E}}(\mathbf{r}_1)\hat{\mathbf{d}}_1 - \hat{\mathbf{E}}(\mathbf{r}_2)\hat{\mathbf{d}}_2. \tag{41}$$

Eliminating the electromagnetic field using the usual Born–Markov approximations leads to a two-atom Liouville equation of the form

$$\begin{aligned}\dot{\varrho} &= -\frac{i}{\hbar}[\hat{H}_0, \varrho] \\ &- \sum_{k,l=1}^{2} \frac{\Gamma(\mathbf{r}_k, \mathbf{r}_l)}{2}(\hat{\sigma}_l^{\dagger}\hat{\sigma}_k\varrho + \varrho\hat{\sigma}_l^{\dagger}\hat{\sigma}_k - 2\hat{\sigma}_k\varrho\hat{\sigma}_l^{\dagger}) \\ &+ \frac{i}{\hbar}\sum_{k,l=1}^{2} \delta\omega(\mathbf{r}_k, \mathbf{r}_l)[\hat{\sigma}_l^{\dagger}\hat{\sigma}_k, \varrho],\end{aligned} \tag{42}$$

where $\hat{\sigma}_l = |1\rangle_{ll}\langle 2|$ is the atomic flip operator of the lth atom from the lower state $|1\rangle$ to the upper state $|2\rangle$. The second and third terms in Eq. (42) describe the spontaneous emission and Lamb shift of the two individual atoms with decay rates $\Gamma(\mathbf{r}_i, \mathbf{r}_i)$ and respective level shifts $\delta\omega(\mathbf{r}_i, \mathbf{r}_i)$, $(i = 1, 2)$. However, they also contain terms describing the radiative interaction between the atoms containing a dissipative cross coupling proportional to $\Gamma(\mathbf{r}_1, \mathbf{r}_2)$ and a conditional level shift proportional to $\delta(\mathbf{r}_1, \mathbf{r}_2)$. The single-atom and cross-coupling rates are given by an expression similar to Eq. (20):

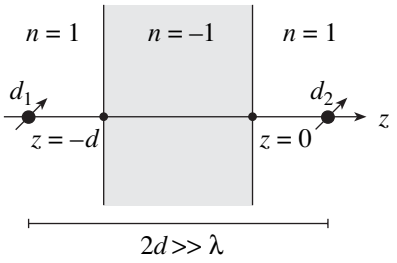

Fig. 9. Two atoms put at the focal points of a Veselago–Pendry lens with $n = -1$. Focal points are all pairs of positions at the two sides of the slab with distance $2d$. The spatial regions $z > 0$ (vacuum), $-d \le z \le 0$ (LHM), and $z < -d$ (vacuum) are denoted by the numbers 0, 1, and 2, respectively.

$$\Gamma(\mathbf{r}_k, \mathbf{r}_l) = \frac{2\omega_A^2 d_i d_j}{\hbar\varepsilon_0 c^2}\text{Im}[G_{ij}(\mathbf{r}_k, \mathbf{r}_l, \omega_A)]. \tag{43}$$

The level shifts read

$$\delta\omega(\mathbf{r}_k, \mathbf{r}_l) = \frac{d_i d_j}{\hbar\pi\varepsilon_0}\mathcal{P}\int_0^{\infty} d\omega \frac{\omega^2}{c^2}\frac{\text{Im}[G_{ij}(\mathbf{r}_k, \mathbf{r}_l, \omega)]}{\omega - \omega_A}. \tag{44}$$

The single-atom Lamb shift $\delta\omega(\mathbf{r}_i, \mathbf{r}_i)$ is not accurately described within the present theory and will be ignored in the following. One recognizes from Eqs. (43) and (44) that the radiative interaction between the two atoms is determined by the imaginary part of the retarded Green function between the positions $\mathbf{r}_1$ and $\mathbf{r}_2$ of the two atoms. In free space, the value of $\mathbf{G}$ rapidly decreases if the relative distance $|\mathbf{r}_1 - \mathbf{r}_2|$ becomes larger than the transition wavelength λ. Consequently, the radiative interaction is negligible except for very small distances. As will be shown now, this situation changes if the atoms are put at the focal points of a Veselago–Pendry lens.

In order to see the effect of the radiative coupling, it is convenient to use as a basis for the two-atom system, besides the total ground state $|11\rangle$ and the doubly-excited state $|22\rangle$, the symmetric and antisymmetric combinations of one atom being excited ($|2\rangle$) and one atom being in its ground state ($|1\rangle$):

$$|s\rangle \equiv \frac{1}{\sqrt{2}}(|12\rangle + |21\rangle), \tag{45}$$

$$|a\rangle \equiv \frac{1}{\sqrt{2}}(|12\rangle - |21\rangle). \tag{46}$$

In terms of these basis states, we arrive at the following density-matrix equation:

$$\dot{\rho}_{22} = -2\Gamma_{11}\rho_{22}, \tag{47}$$

$$\dot{\rho}_{ss} = -(\Gamma_{11} + \Gamma_{12})\rho_{ss} + (\Gamma_{11} + \Gamma_{12})\rho_{22}, \tag{48}$$

$$\dot{\rho}_{aa} = -(\Gamma_{11} - \Gamma_{12})\rho_{aa} + (\Gamma_{11} - \Gamma_{12})\rho_{22}, \quad (49)$$

$$\dot{\rho}_{11} = +(\Gamma_{11} + \Gamma_{12})\rho_{ss} + (\Gamma_{11} - \Gamma_{12})\rho_{aa}, \quad (50)$$

where we have disregarded the level shifts and where Γ_{ij} is an abbreviated notation for $\Gamma(\mathbf{r}_i, \mathbf{r}_j)$. One recognizes from the above equations that the decay channels through the symmetric and antisymmetric superpositions differ by the cross-coupling contribution $\pm\Gamma_{12}$ if the two atoms are in free space at the same point $\Gamma_{12} = \Gamma_{11} = \Gamma_{22}$. In this case, the antisymmetric state does not decay at all, while the symmetric one decays with twice the single-atom decay rate. This is the situation of Dicke sub- and superradiance [13].

Let us now calculate the rates Γ_{11}, Γ_{22} and Γ_{12}, i.e., the imaginary part of the Green function for the situation of Fig. 9. Since at the boundary between vacuum ($n = +1$) and LHM ($n = -1$) there is no reflection, i.e., $R^{\mathrm{TE}} = R^{\mathrm{TM}} = 0$, one finds, for the case of both positions being on the left side of the lens (region "0"),

$$\mathrm{Im}[G^{00}_{\mu\mu}(\mathbf{r}, \mathbf{r})] = \mathrm{Im}\frac{i}{8\pi^2}\int_0^\infty dk_\perp \frac{k_\perp}{\sqrt{k^2 - k_\perp^2}} \times\left(\left(1 + R^{\mathrm{TE}} e^{i\sqrt{k^2 - k_\perp^2}d}\right)\pi\right. \quad (51)$$

$$\left. + R^{\mathrm{TM}} e^{i\sqrt{k^2 - k_\perp^2}d}\pi\left(\frac{k_\perp^2}{k^2} - 1\right) + \pi\left(1 - \frac{k_\perp^2}{k^2}\right)\right) = \frac{k}{6\pi}.$$

The same result holds, of course, for both positions being on the right side of the lens (region "2"). A corresponding calculation for $\mathbf{r}$ being on the left side (region "0") and $\mathbf{r}'$ being the other focal point of the lens $\mathbf{r} + 2d\mathbf{e}_z$ yields

$$\mathrm{Im}[\mathbf{G}^{20}_{\mu\mu}(\mathbf{r}, \mathbf{r} + 2d\mathbf{e}_z)] = \mathrm{Im}\frac{i}{8\pi^2}\int_0^\infty dk_\perp \frac{k_\perp}{\sqrt{k^2 - k_\perp^2}} \times e^{i2\sqrt{k^2 - k_\perp^2}d}\left(T^{\mathrm{TE}}\pi + T^{\mathrm{TM}}\pi\left(1 - \frac{k_\perp^2}{k^2}\right)\right) = \frac{k}{6\pi}, \quad (52)$$

where $T^{\mathrm{TE}} = T^{\mathrm{TM}} = e^{i(k_{1z} - k_z)d}$ and $k_{1z} = -k_z$. Equations (35) and (36) have been used. Thus, we recognize that the imaginary part of the Green function between the two focal points is identical to that at the same position. As a consequence, $\Gamma_{12} = \Gamma_{11}$ and there is perfect sub- and superradiance, despite the fact that the distance between the focal points can be much larger than the resonance wavelength. Figure 10 illustrates the dependence of the ratio Γ_{12}/Γ_{11} on the spatial displacement of the second atom from the focal point of the first.

One recognizes from Fig. 10 that, for the imaginary part of the Green function of the ideal Veselago–Pendry lens, the following holds:

$$\mathrm{Im}[\mathbf{G}(\mathbf{r} - 2d\mathbf{e}_z, \mathbf{r}, \omega)] = \mathrm{Im}[\mathbf{G}(\mathbf{r}, \mathbf{r}, \omega)]. \quad (53)$$

It should be noted here that a relation similar to Eq. (53) does not exist for the real part of the Green function. If this were true, then the electric field pattern at the two focal points would be identical, in violation of Maxwell's equations. It should also be noted that relation (53) holds only within a certain range of frequencies ω, due to the necessarily dispersive nature of the LHM. The limitations arising from this will be discussed in the following section.

6. LIMITATIONS

In Sections 4 and 5, two systems involving perfect left-handed materials were discussed. We here turn to the following question: what are the limitations of the observed effects under more realistic conditions, i.e., when taking into account absorption losses, a finite transversal extension of the LHM slab, and dispersion of the medium?

6.1. Absorbing LHMs

First of all, to describe a more realistic LHM, one has to take absorption into account. This can easily be done by substituting the refractive index $n = -1$ of the perfect LHM by $n = -1 + in_I$, i.e., by adding an imaginary part.

For the mirror system of Section 4, Fig. 11 shows the dependence of $\Gamma^{\parallel}/\Gamma_0$ on the absorption coefficient n_I for different thicknesses of the LHM. As can be seen, the suppression of the spontaneous emission for atomic dipoles parallel to the mirror decreases with increasing absorption, as was expected. The sensitivity to absorption is approximately exponential in $n_I d$.

In Fig. 12, the same is shown for the system with the lens. As was expected, Γ_{12}/Γ_{11}, and, therefore, the effect of the sub/superradiance is reduced with increasing absorption coefficients n_I. The dependence on the thickness of the lens is again exponential.

6.2. Finite Transverse Extension of the LHM

In experimental implementations, the slab of LHM will always have a finite transversal extension. We therefore analyze here the dependence of the LHM-induced effects on the transversal radius of the medium. The thickness of the LHM is denoted by d, and the transverse extension by a (Fig. 13). Because of the finite radius, the 1D character of the geometry is no longer given, and the Green function cannot be calculated analytically. A numerical solution for the Green function is also very difficult. Noting, however, that only propagating modes with $k_\perp \le k$ contribute to the

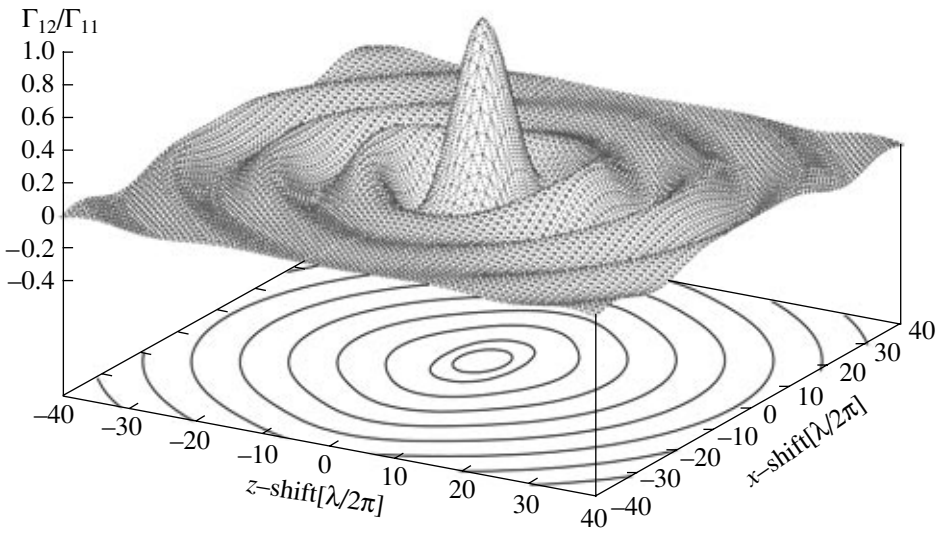

Fig. 10. Γ_{12}/Γ_{11} as a function of the spatial shift, parallel "x" and orthogonal "z" to the surface of the LHM, of one atom out of the focus of the other one. In the focal point (0, 0), perfect sub- and superradiance is obtained. Here, the dipoles of both atoms are oriented in the x direction.

imaginary part of the Green functions, one can obtain an estimate of the effect in the short-wavelength or ray-optics limit ($d \gg \lambda$).

For the system with the mirror, this means that, for the integrand over $k_\perp$ in the definition of the Green function (Eq. (31)), one should use the expression for $\mathbf{G}^{00}_{\mathrm{LHM}}$ only for values

$$k_\perp \le k \frac{\frac{a}{d}}{\sqrt{1+\left(\frac{a}{d}\right)^2}}. \qquad (54)$$

This corresponds to angles α of the propagating modes that are less than $\sin\alpha = \frac{a}{\sqrt{a^2+d^2}} = k_\perp/k$ (Fig. 13). For larger angles, the result depends strongly on whether or not the mirror also has a finite transversal extension. When the mirror has the same transversal radius a, one has to use $\mathbf{G}_{\mathrm{vac}}$ (dashed line in Fig. 14); otherwise, the expression for $\mathbf{G}^{00}_{\mathrm{LHM}}$ needs to be taken, but with $n = 1$ substituted for $n = -1$ (solid line Fig. 14).

For the system with the lens, an estimate of the effect of a finite transverse radius is given here only for

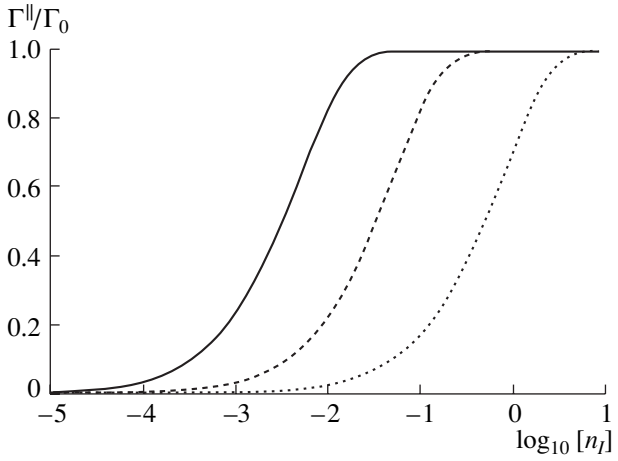

Fig. 11. $\Gamma^{\parallel}/\Gamma_0$ as a function of the imaginary part of the refractive index n_I for $\mathrm{Re}[n] = -1$ and different thicknesses d of the lens, $d = 100\lambda/2\pi$ (solid line), $d = 10\lambda/2\pi$ (dashed), and $d = 1\lambda/2\pi$ (dotted).

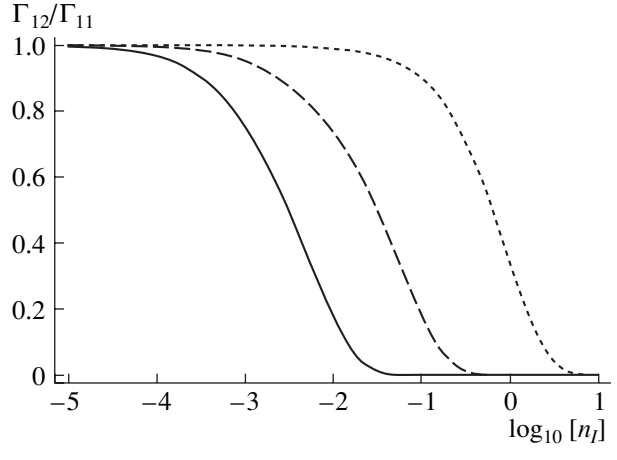

Fig. 12. Γ_{12}/Γ_{11} as a function of the imaginary part of the refractive index n_I for $\mathrm{Re}[n] = -1$ for different thicknesses d of the lens, $d = 100\lambda/2\pi$ (solid line), $d = 10\lambda/2\pi$ (dashed), and $d = 1\lambda/2\pi$ (dotted).

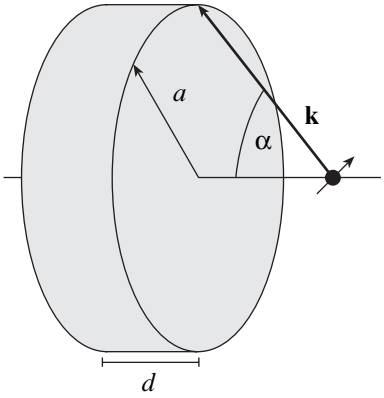

Fig. 13. Finite extension of the LHM in the transverse direction.

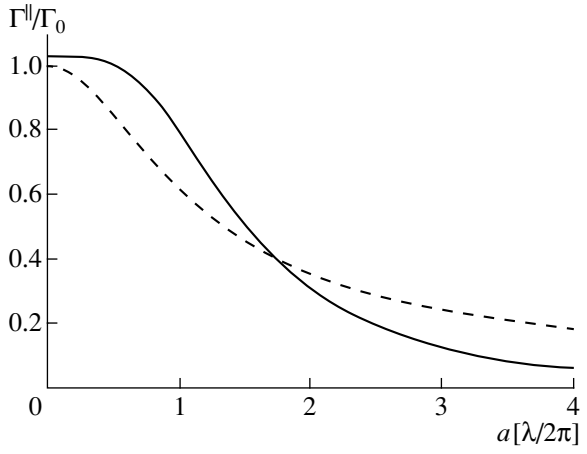

Fig. 14. $\Gamma^{\|}/\Gamma_0$ as a function of the transversal radius a of the LHM with thickness $d = 3\frac{\lambda}{2\pi}$. The mirror itself was assumed to be infinitely extended (solid) or of the same dimension as the LHM (dashed).

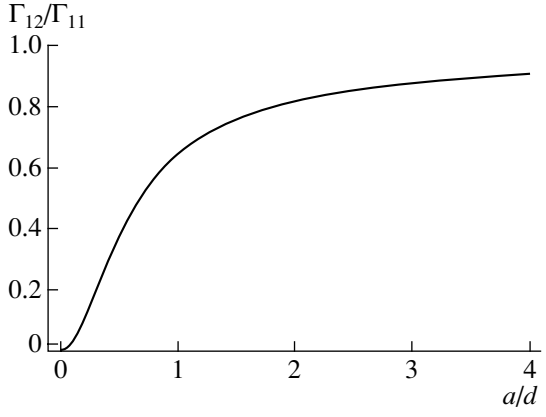

Fig. 15. Γ_{12}/Γ_{11} as a function of the normalized transversal radius a/d.

a symmetric setup, i.e., when the distance of both atoms to the surface of the lens is $d/2$. Under this assumption, the desired result can be obtained more easily than for the mirror case, since the atoms are macroscopically separated. In this case, the Green function $\mathbf{G}_{\mathrm{vac}}(\mathbf{r}_1, \mathbf{r}_2)$ is essentially zero, and the integration over $k_\perp$ can effectively be limited to the values

$$k_\perp \leq k\frac{\frac{a}{d}}{\sqrt{\frac{1}{4}+\left(\frac{a}{d}\right)^2}}, \tag{55}$$

with the integrand being the usual expression for $\mathbf{G}^{20}(\mathbf{r}_1, \mathbf{r}_2)$. As can be seen from Fig. 15, even for a moderate ratio a/d a sub/superradiance that is close to 100% can be obtained.

6.3. Dispersion Effects

The spontaneous emission is given by the imaginary part of the retarded Green tensor at the transition frequency (Eq. (20)). Therefore, the predictions of Sections 4 and 5 hold as long as the frequency range with $n = -1$ is large compared to the natural linewidth Γ.

The previous discussion suggests that, if the LHM used for the lens in Section 5 has arbitrarily small losses in the frequency range of interest and also has a sufficient large transversal extension, sub- and superradiance is possible for two atoms at an arbitrary distance. For causality reasons this is, of course, not possible. The resolution of this seeming contradiction lies in the necessary dispersion of a left-handed material, as was discussed in Section 2. The positivity of the electromagnetic energy in a lossless LHM requires that $\frac{d}{d\omega}(\omega\mathrm{Re}[\epsilon(\omega)]) \geq 0$ and $\frac{d}{d\omega}(\omega\mathrm{Re}[\mu(\omega)]) \geq 0$, which implies the following for $n(\omega_0) = -1$:

$$\frac{d}{d\omega}n(\omega_0) \geq \frac{1}{\omega_0}. \tag{56}$$

As a consequence of the dispersion of the refractive index, the frequency window $\Delta\omega$ over which $\mathbf{G}^{20}(\omega) \approx \mathbf{G}^{00}(\omega)$ narrows with increasing thickness of the lens. When $\Delta\omega$ becomes comparable to the natural linewidth of the atomic transitions Γ_{11}, the Markov approximation implicitly used for the derivation of Eq. (42) is no longer valid. To give an estimate of when this happens, we note from Eqs. (32)–(37) that, for $d \gg \lambda$, the term in $\mathbf{G}^{20}$ that is most sensitive to dispersion is the exponential factor $e^{i\mathbf{K}\cdot(\mathbf{r}-\mathbf{r}')}e^{i(k_{1z}-k_z)d}$. Taking into account a linear dispersion of $n(\omega)$ in this exponential factor according to $n = -1 + \alpha(\omega - \omega_0)$, with a real value of α, while

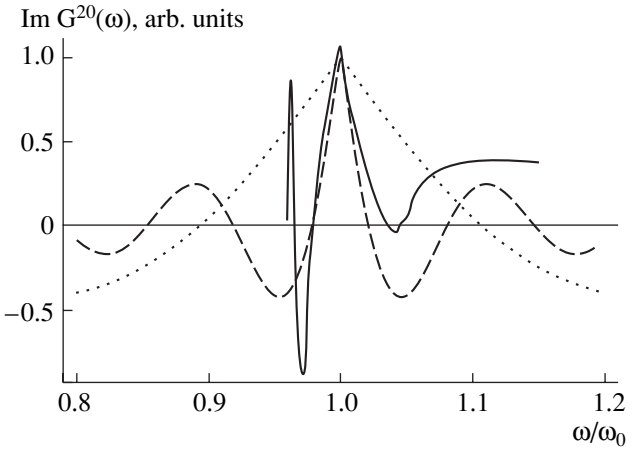

Fig. 16. Im[$\mathbf{G}^{20}(\omega)$] following from Eq. (57) for lossless LHM with $n = -1 + \alpha(\omega - \omega_0)$ for $\alpha = 45/\omega_0$ for $dk_0 = 1$ (dashed) and 0.2 (dotted). Also shown is the numerically calculated spectrum for a specific causal model for $n(\omega)$ with resonances of $\varepsilon(\omega)$ and $\mu(\omega)$ below ω_0. $n(\omega)$ was chosen such that $\mathrm{Re}[n(\omega_0)] = -1$ and $\alpha = 45/\omega_0$. The central structure is well represented by the linear-dispersion approximation (Eq. (57)). Furthermore, a narrowing of the spectral width with increasing thickness is apparent.

keeping the resonance values for T^{TE}, T^{TM} and R^{TE}, R^{TM}, one finds the following for the Green tensor:

$$\mathrm{Im}[\mathbf{G}^{20}(\omega)] = \frac{k}{8\pi}\mathrm{Re}\left[\int_0^1 d\xi(1+\xi^2)e^{i\frac{dk_0}{\xi}\alpha(\omega-\omega_0)}\right]\hat{\mathbf{1}}. \quad (57)$$

As can be seen from Fig. 16, the spectral width $\Delta\omega$ of the Green function is, in this approximation, of order

$$\Delta\omega \approx (k_0 d\alpha)^{-1}. \quad (58)$$

Since as mentioned above, for a lossless LHM, $\alpha \geq 1/\omega_0$, one arrives at

$$\Delta\omega \leq c/d. \quad (59)$$

This leads to an upper bound on the distance of the atoms. The requirement $\Delta\omega \gg \Gamma_{11}$ leads to

$$d \ll \frac{c}{\Gamma_{11}}. \quad (60)$$

This condition can easily be understood. It states that the distance between the two atoms must be small enough such that the travel time of a photon from one atom to the other is small compared to the free-space radiative lifetime.

7. SUMMARY

In the present paper, we have studied the interaction of an isolated atom or a pair of atoms with the quantized electromagnetic field in the presence of media with negative indices of refraction. An expression for the rate of spontaneous emission of an atom embedded in a LHM was derived (see also [15]), which is a generalization of the Glauber–Lewenstein result [17] to magnetodielectric media. We have shown that the negative optical path length occurring in left-handed materials can be used to induce strong QED effects over large distances, which in vacuum otherwise occur only on subwavelength-length scales. Considering an isolated atom in front of a perfect mirror with a layer of LHM of thickness d, we found an interesting modification of the Purcell effect. Spontaneous emission was found to be completely suppressed for an atom placed at a distance $2d$ from the mirror in vacuum. It was shown, furthermore, that two atoms at the focal points of a Veselago–Pendry lens that consists of a parallel slab of ideal LHM display perfect sub- and superradiance. A principle limitation of the involved length scales is given only by the intrinsic dispersion of left-handed materials, which prevents strong radiative coupling over distances larger than the propagation distance of light, corresponding to the free-space radiative-decay time. We anticipate that the unusual property of LHM of leading to negative optical path length will have a number of interesting applications, e.g., zero-optical-length resonators. On the other hand, much of the present discussion is still only of academic interest, since no low-loss negative-index materials are known for the interesting case of optical frequencies.

REFERENCES

1. E. M. Purcell, Phys. Rev. **69**, 681 (1946).
2. D. Kleppner, *Atomic Physics and Astrophysics*, Ed. by M. Chretien and E. Lipworth (Gordon and Breach, New York, 1971).
3. R. G. Hulet, E. S. Hilfer, and D. Kleppner, Phys. Rev. Lett. **55**, 2317 (1985).
4. P. Goy, J. M. Raimond, M. Gross, and S. Haroche, Phys. Rev. Lett. **50**, 1903 (1983).
5. A. G. Vaidvanathan, W. P. Spencer, and D. Kleppner, Phys. Rev. Lett. **47**, 1592 (1981).
6. P. Dobiasch and H. Walther, Ann. Phys. (Paris) **10**, 825 (1985).
7. K. H. Drexhage, in *Progress in Optics*, Ed. by E. Wolf (North-Holland, Amsterdam, 1974).
8. Y. Yamamoto, Opt. Commun. **80**, 337 (1991).
9. E. Yablonovich, Phys. Rev. Lett. **58**, 2059 (1987).
10. S. John and T. Quang, Phys. Rev. A **50**, 1764 (1994).
11. V. G. Veselago, Sov. Phys. Usp. **10**, 509 (1968).
12. J. B. Pendry, Phys. Rev. Lett. **85**, 3966 (2000).
13. R. H. Dicke, Phys. Rev. **93**, 99 (1954).
14. G. Nienhuis and C. Th. J. Alkemade, Physica C (Amsterdam) **81**, 181 (1976).
15. Ho Trung Dung, S. Y. Buhmann, L. Knöll, *et al.*, Phys. Rev. A **68**, 043816 (2003).
16. J. Kästel, Diploma Thesis (TU Kaiserslautern, 2003).
17. R. J. Glauber and M. Lewenstein, Phys. Rev. A **43**, 467 (1991).
18. L. Knöll, S. Scheel, and D. G. Welsch, in *Coherence and Statistics of Photons and Atoms,* Ed. by J. Perina (Wiley, New York, 2001).
19. L. W. Li, P. S. Kooi, M. S. Leong, and T. S. Yeo, IEEE Trans. Microwave Theory Tech. **42**, 2302 (1994).
20. H. Morawitz, Phys. Rev. **187**, 1792 (1969).
21. L. Tsang, J. A. Kong, and R. T. Shin, *Theory of Microwave Remote Sensing* (Wiley, New York, 1985).